Applied Occupational and Environmental Hygiene

ISSN: 1047-322X (Print) 1521-0898 (Online) Journal homepage: https://www.tandfonline.com/loi/uaoh20

Vapor/Solid Chemisorption Model for Passive Sampling of Aldehydes

Shih-Wei Tsai & Shane S. Que Hee

To cite this article: Shih-Wei Tsai & Shane S. Que Hee (2002) Vapor/Solid Chemisorption Model for Passive Sampling of Aldehydes, Applied Occupational and Environmental Hygiene, 17:8, 551-560, DOI: 10.1080/10473220290095826

To link to this article: https://doi.org/10.1080/10473220290095826

Published online: 30 Nov 2010.

Applied Occupational and Environmental Hygiene
Volume 17(8): 551–560, 2002

1047-322X/02 $12.00 + .00
DOI: 10.1080/1047322029009582 6

Vapor/Solid Chemisorption Model for Passive Sampling of Aldehydes

Shih-Wei Tsai* **and Shane S. Que Hee**
Department of Environmental Health Sciences and UCLA Center for Occupational and Environmental Health, UCLA School of Public Health, Los Angeles, California

The vapor-phase chemisorption isotherms of valeraldehyde (*n*-valeraldehyde; 1-pentanal) and acrolein (2-propenal) above the critical face velocity (7.5 cm/s) were investigated at 25°C and 36 percent relative humidity (RH) for a passive air sampling pellet of 10 percent O-(2,3,4,5,6-pentafluorobenzyl)-hydroxylamine hydrochloride (PFBHA) on Tenax TA solid sorbent (80/100 mesh). A dynamic air dilution system with syringe pumps generated the vapor concentrations and humidity for the exposure chamber. The O-oxime derivatives were desorbed with hexane for gas chromatographic analysis on a nonpolar capillary column and electron capture detection. The pellet capacity was about 30 μmoles. Adsorption of valeraldehyde was best fitted by a Langmuir or Brunauer-Emmett-Teller (BET) I model. That for acrolein was described best by a Dubinin-Radushkevich model. A microporosity model explained why all the classical isotherms described the chemisorption behavior. An activated extrinsic precursor was suggested to facilitate the addition reaction by production of a protonated intermediate formed by the transfer of a proton to the aldehyde from an activated reaction site consisting of at least 2 PFBHA molecules.

Keywords Chemisorption, Adsorption, Isotherm, Aldehyde, Passive Sampling, Diffusion

Aldehydes are important industrial chemicals, and irritant products of combustion (for example, from automobile exhaust) and of oxidation (for example, in photochemical smog).[1–3] Formaldehyde, acetaldehyde, crotonaldehyde, and furfural are also animal carcinogens.[2]

Air sampling methods for aldehydes often use solid sorbents with pumps.[1–8] Passive samplers having no pump and sampling by diffusion are convenient, light, and inexpensive; many can be deployed simultaneously.[9] Commercial solid sorbent passive samplers for the lower aldehydes are usually based on 2,4-dinitrophenylhydrazine (2,4-DNPH).[10–13] Our research group has reported on the aldehyde chemisorption derivatives of O-(2,3,4,5,6-pentafluoro)benzylhydroxylamine hydrochloride (PFBHA) in dynamic[7,8] and passive[14,15] air sampling with PFBHA-coated Tenax at ppbv-ppmv concentrations. Temperature and relative humidity (RH) do not affect sampling efficiency and capacity,[7,8,14,15] unlike in the 2,4-DNPH methods. Since Tenax TA has a very low bed volume for water vapor, RH effects on bed capacities of organic adsorbates are minimal.[16] Aldehyde vapors are also physically adsorbed by Tenax TA.[17,18] Chemisorption of aldehydes with PFBHA coated on a fused silica fiber is also used[19,20] in solid phase microextraction (SPME)[21] of air headspace analysis above aqueous solutions.

Chemisorption often obeys a Langmuir adsorption isotherm (Brunauer-Emmett-Teller [BET] Type I) model[22] that also fits many physical adsorption processes. The aim of the present study was to use the PFBHA-coated Tenax TA system as a model passive chemisorptive system to investigate classical isotherm utility to define capacity parameters for aldehyde chemisorption.

EXPERIMENTAL SECTION

Diffusion Theory and Adsorption

For a cylindrical open tube,[14,15] a sampling constant $k_{analyte}$ is defined for the analyte in air through Fick's first law of diffusion, Eq. (1):

$$dm_{analyte}/dt = (DA/L)(C_{air} - C_{surf}) = k_{analyte}\ (C_{air} - C_{surf}) \quad [1]$$

where $dm_{analyte}/dt$ is the analyte mass sampling rate or mass transfer rate, weight/time; D is the analyte diffusion coefficient in air, cm^2/s; A is the cross-sectional area of the sampling surface, cm^2; L is the effective diffusion path length, cm; C_{air} is the air concentration of the analyte, weight/cm^3; C_{surf} is the air concentration of analyte at the sampling surface in the same units as C_{air}; and $k_{analyte} = DA/L$ is the analyte sampling constant, cm^3/time.

*Presently in the Department of Occupational Safety and Health, China Medical College, Taichung, Taiwan.

D depends on molecular weight M and temperature T as in Eq. (2):[23,24]

$$D = 0.001\, T^{1.75}(1/M_{air} + 1/M_{analyte})^{0.5}/ \left\{p_e\left[v_{air}^{1/3} + v_{analyte}^{1/3}\right]^2\right\} \quad [2]$$

where D is the diffusion coefficient of analyte in air in cm^2/s; T is temperature, K; M_{air} and $M_{analyte}$ are molecular weights for air and the analyte respectively, g/mol; p_e is the external pressure, bar; v_{air} is the normalized molecular diffusion volume of air, unitless; $v_{analyte}$ is the normalized molecular diffusion volume of analyte, being the sum of the normalized diffusion volumes of the component atoms, unitless.

C_{surf} is important near saturation, but is negligible if chemisorption is fast and efficient and the product is much less volatile than the initial physically adsorbed species. Hence:

$$dm_{analyte}/dt \cong (DA/L)C_{air} \cong k_{analyte}C_{air} \quad [3]$$

The chemisorptive reaction can be represented generally as:

$$\text{a analyte} + \text{b reactant} \rightarrow \text{c product 1} + \text{d product 2} \quad [4]$$

where a, b, c, and d are the moles of analyte, reactant, product 1, and product 2, respectively.

The overall reaction for an aldehyde with one carbonyl group R—CHO (R is H, alkyl, or aryl) and PFBHA R′—O—NH_2.HCl (R′ is the 2,3,4,5,6-pentafluorobenzyl group) is:

$$\underset{\text{Aldehyde}}{R\text{—}CHO} + \underset{\text{PFBHA}}{R'\text{—}O\text{—}NH_2.HCl} \leftrightarrow \underset{\text{O-oxime}}{R'\text{—}O\text{—}N{=}CH\text{—}R} + \underset{\text{Water}}{H_2O} + \underset{\text{Hydrogen chloride}}{HCl} \quad [5]$$

One mole of aldehyde produces one mole of O-oxime product, assuming no side reactions and perfect yield (reaction fractional efficiency $R_e = 1$). For excess PFBHA, the number of moles of O-oxime product measured is then the same as the number of moles of aldehyde reacted, and the rate of product formation (mol/time) equals the aldehyde reaction rate (mol/time). The reacted aldehyde mass transfer rate $dm_{ranalyte}/dt$ in units of mass/time is thus:

$$dm_{ranalyte}/dt = (dm_{product}/dt)(M_{analyte}/M_{product}) \times (1/R_e) = (dm_{product}/dt)(f/R_e) \quad [6]$$

where $M_{product}$ is the molecular weight of the reaction product (the O-oxime); $f = M_{analyte}/M_{product}$.

$dm_{ranalyte}/dt$ in Eq. (6) and $dm_{analyte}/dt$ in Eqs. (1) and (3) are not necessarily equal. Equations similar to Eqs. (1) and (3) can be written for $dm_{ranalyte}/dt$ as:

$$dm_{ranalyte}/dt = (DR_rA/L)(C_{air} - C_{surf}) = R_r k_{analyte}(C_{air} - C_{surf}) = k'_{ranalyte}(C_{air} - C_{surf}) \quad [7]$$

where $k'_{ranalyte} = (DR_rA/L) = R_r\, k_{analyte}$, since not all the physically adsorbed analyte molecules may react, as reflected in R_r, the physically adsorbed fraction that also chemisorbs.

As for Eq. (3) and considering Eq. (6):

$$dm_{ranalyte}/dt \cong (DR_rA/L)C_{air} \cong k_{analyte}\, R_r\, C_{air} \cong k'_{ranalyte}C_{air} \cong (dm_{product}/dt)(f/R_e) \quad [8]$$

The relationship between $dm_{product}/dt$ and C_{air} over a specific sampling time is determined experimentally to define $(k_{analyte}\, R_r\, R_e)/f$ practically, assuming constant R_e and R_r. The useful range for passive sampling is the linear Henry's Law region that Eqs. (3) and (8) reflect. If $C_{surf} \neq 0$, a still usable linear relationship with a non-zero intercept may result, Eqs. (1) and (7). In contrast, adsorption isotherm studies involve C_{air} above the linear region to define bed capacity and the area of the adsorbing sites, and where R_r and R_e may not be constant.

Aldehydes Selected

Acrolein and valeraldehyde were investigated. They are at the extremes of recommended or regulated workplace concentrations for an 8-hr workday: the acrolein permissible exposure limit is 0.1 ppmv; the valeraldehyde time weighted average threshold limit value (TWA-TLV®) is 50 ppmv. The PFBHA O-oximes have also been synthesized.[7,8] Acrolein is a stiff short molecule whereas the long chain of valeraldehyde is flexible.

Materials

Acrolein (97%) and valeraldehyde (99%) were from Aldrich (Milwaukee, WI), as was the GC internal standard, decafluorobiphenyl. Hexane (Optima), methanol (Optima), nitric acid, activated charcoal, molecular sieves, and Drierite were from Fisher Scientific. PFBHA was from Lancaster Laboratories. Tenax TA (80/100 mesh; specific surface area, 35 m^2/g)[18] was from Alltech (Deerfield, IL), and it was purified and dried as detailed elsewhere.[14,15] Helium, nitrogen, and 95 percent methane/argon were ultrapure grade from Alphagaz.

Equipment

The detailed list of laboratory equipment, operation of the air dilution system of Figure 1, and preparation of the passive sampler (Figure 2) are provided elsewhere.[14,15]

A Hewlett-Packard 5890 GC/^{63}Ni-ECD utilized a 30-m × 0.32-mm ID 1-μm DB-1701 chemically bonded fused-silica capillary column (J&W Scientific) at 3.0 ± 0.4 ml/min of 95 percent methane/argon. The injector and detector temperatures were 250°C. The column temperature program for valeraldehyde was: solvent delay, 5 min at 105°C; 105°C for 0.5 min; 105°C to 180°C at 10°C/min; and holding 4 min. The program for acrolein was the same except 105°C to 230°C at 10°C/min, and holding 9 min were used for the last two steps. The areas of both *E*- and *Z*-isomers were utilized for quantitations. Linear

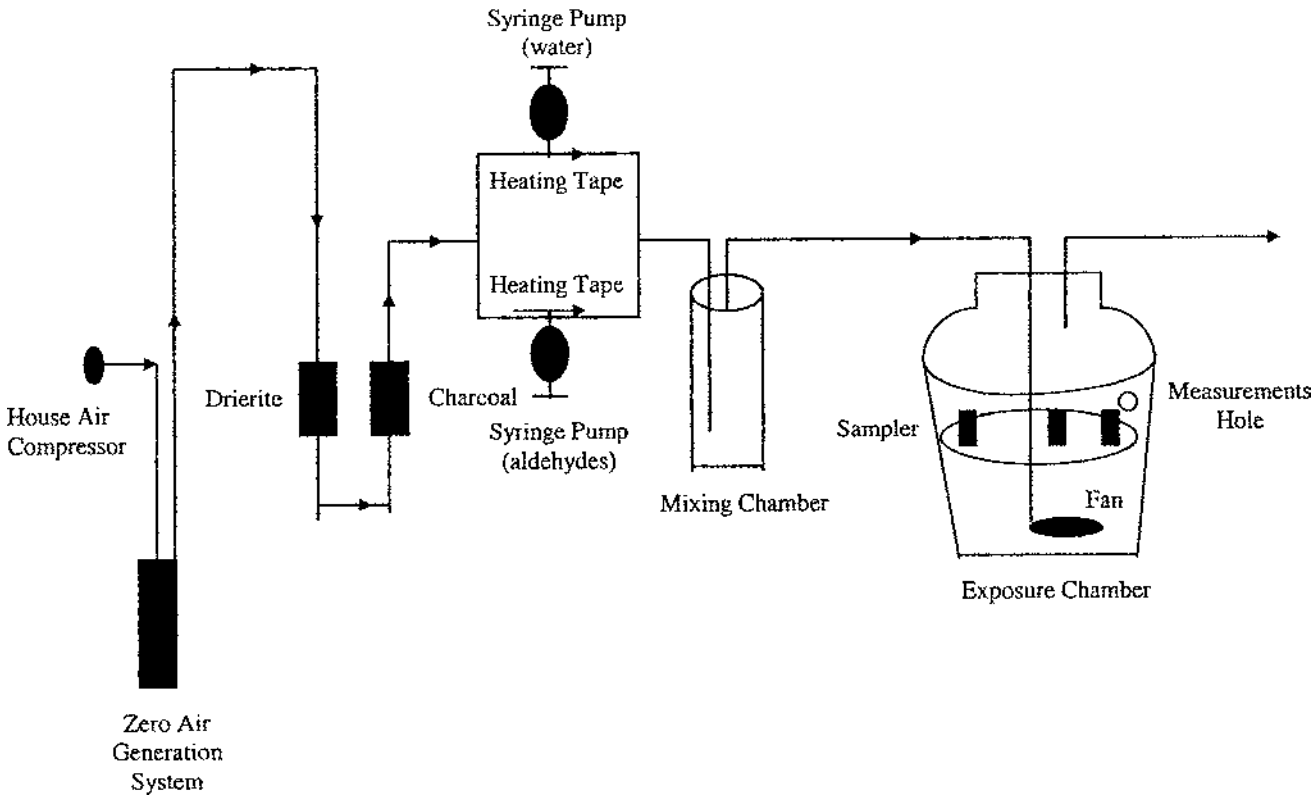

FIGURE 1
Aldehyde vapor generation and exposure chamber system schematic.

ranges were 200 to 1500 pg valeraldehyde equivalent and 180 to 3500 pg acrolein equivalent. Injections of 2-μl were used.

Desorption Efficiency of O-Oximes

A volume of 50 μl of hexane solution containing the theoretical mass of O-oxime formed after sampling 8 hours of exposure at the PEL or TLV was spiked onto the pellet. The spiked pellet was held overnight in a desiccator containing Drierite before desorption with 2.0 ml hexane at room temperature for 2 hr with ultrasonication for 0.2 min every half hour before GC/ECD analysis. All experiments were in triplicate.

Reaction Efficiency/O-Oxime Recovery for Wet Spiking of Aldehyde and Capacity Studies

A weight of 1.338 mg of liquid valeraldehyde (2 TLV $\times$ 8 hr mass) was spiked directly onto the sampling pellet. Acrolein was spiked at 1.81 μg (2 PEL $\times$ 8 hr) in 50 μl of methanol. GC/ECD analyses were then performed on desorption of the PFBHA O-oximes after an overnight holding period in a desiccator. Liquid spiking capacities were also determined at higher aldehyde concentrations until saturation. PFBHA aldehyde pure standards were used for quantification. All experiments were in triplicate.

Vapor Exposures

Triplicate exposures were performed at $(25 \pm 1)^{\circ}$C, (36 ± 2) percent RH, and 51 ft/min (25.5 cm/s), the latter being above the critical face velocity of 15–20 ft/min (7.6–10.0 cm/s). Direct-reading photoionization detection (PID; 11.6 eV lamp; H-Nu Model 101) of the exposure chamber vapor concentration occurred >1 ppmv. The total ppm-hr was obtained by summing the area under the PID ppmv versus time plots. The half-time to maximum concentration was 5–10 min, and to baseline from the maximum was 10–15 min. Acrolein TWA concentrations over the exposure period were obtained by the PFBHA dynamic sampling method[7] at 50 ml/min pump flow rate with 3 ml hexane desorption, and GC/ECD analysis.

The usual protocol involved generating at least 0, 8.0, and 16 times the TLV concentration over one hour of exposure, and then continuing with higher concentrations increasing twofold in 1-hr exposures to reach pellet capacity, as signified by constant O-oxime formed. Previous work has shown sampler equivalence for a TLV concentration exposed for 8 hr with that for 8 times the TLV concentration exposed for 1 hr.[14] Passive samplers were desorbed with hexane as for the spiking studies, followed by GC/ECD analysis.

Adsorption Isotherms

The aldehyde equivalent moles desorbed per unit weight of sorbent q_A was first calculated from the moles of determined O-oxime as indicated in Eqs. (5) and (6), correcting for the measured desorption and sampling efficiencies (mol/g solid). Other key parameters calculated were: C_A, the concentration

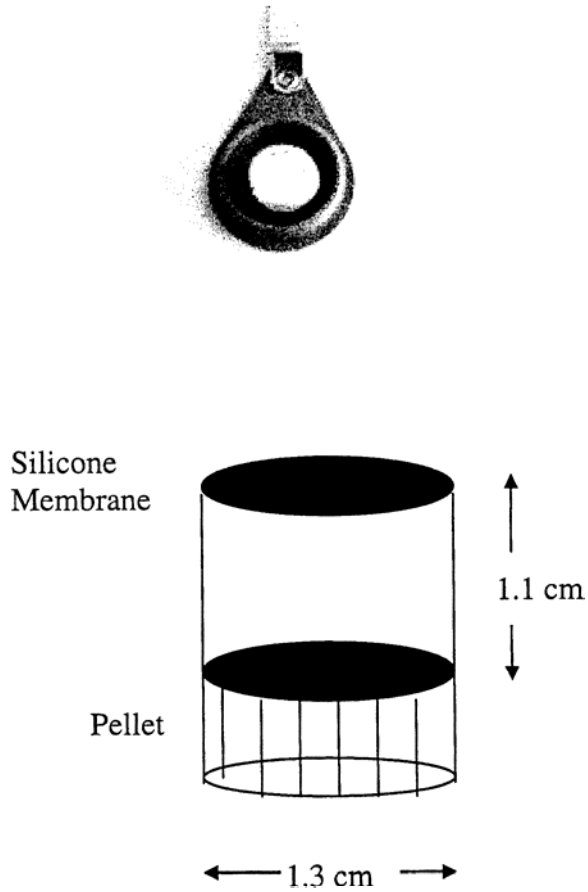

FIGURE 2
Cross section of the passive sampler.

(mol/cm^3) of aldehyde in the air corresponding to its air partial pressure p (assuming the Ideal Gas law p/RT where R is the gas constant and T in K) that produced its O-oxime product q_A (mol/g) over the exposure time; C_A^*, the air concentration (mol/cm^3) that corresponds to the vapor pressure p^* at temperature T (in K), corrected for T by the Clausius-Clapeyron equation; and the relative pressure $z = p/p^* = C_A/C_A^*$.

The linearization equations and parameters for each classical isotherm are provided in Table I.[22] A BET isotherm applies for a linear plot of $z/([1-z]q_A)$ versus z. The BET Type I isotherm is also the Langmuir isotherm (linear C_A/q_A versus C_A plot). For a Freundlich isotherm, ln q_A versus ln C_A is linear. For the Dubinin-Radushkevich (D-R) isotherm, ln ($q_A = W/V_l$) versus $R^2T^2(\ln^2 z^{-1})$ is linear (W is the observed filled volume of adsorption sites, ml/g; V_l is the liquid molar volume, ml/mole; R is the gas constant; and T is in K). Other parameters calculated included the specific analyte bed capacity n_m (mol/g sorbent), the specific analyte bed volume capacity v_m (μl/g), and analyte adsorption energies in kJ/mol.

Statistics

Analysis of variance type I and II procedures were used to detect significant differences and interactions at $p \leq 0.05$.[26] Means were also compared with Student's t tests at $p \leq 0.05$.[26] Linear regressions were performed with an SAS statistical package that also provided standard deviations of the slope and intercept as well as correlation coefficients R and p values.

RESULTS AND DISCUSSION

Desorption Efficiencies and Effects of Physical Parameters

The desorption efficiencies for wet spiking of PFBHA oximes of valeraldehyde and acrolein at 8 × TLV concentration equivalent were 95.6 ± 5.4 percent and 107.2 ± 5.4 percent, respectively, not significantly different from 100 percent at $p \leq 0.05$ for the same relative standard deviations (RSD). The respective recoveries after wet spiking of aldehyde well below saturation were 94.0 ± 3.6 percent and 98.5 ± 7.3 percent. The acrolein vapor moles chemisorbed assuming $R_e = 1$ were not significantly different from the moles predicted from Eqs. (2) and (3), being 96.8 ± 3.4 percent from 30 experiments at 10 different conditions at vapor concentrations 0.08–1.6 ppmv for 1 hr[14] or $(dm_{ranalyte}/dt)/(dm_{analyte}/dt) = 0.968 \pm 0.034$, near 1.0. Similarly, the ratio for valeraldehyde vapor at 40–800 ppmv for 1 hr was 0.750 ± 0.019. The D calculated from Eq. (2) for valeraldehyde may not be for the normal-chain isomer because the Fuller-Schettler-Giddings model[23] does not distinguish skeletal isomers. Since normal chain isomers have the lowest vapor pressures of isomers, the corresponding D may be the lowest for the straight-chain isomer. Thus, the calculated D may be too high, and the calculated R_r too low. This illustrates why experimental D have to be determined.

Capacities

Figure 3 shows the vapor isotherms as moles of product per 150 mg pellet from Eq. (6) versus aldehyde moles expected to react from Eq. (3) using calculated D from Eq. (2). The slopes are not close to 1.0 at these high air concentrations. Figure 3 shows the same asymptotes for both aldehydes at 29–33 μmol.

The measured vapor and wet spiking pellet capacities were 32.9 ± 3.5 and 28.0 ± 4.8 μmol valeraldehyde, respectively. The corresponding data for acrolein were 29.1 ± 2.8 and 25.9 ± 5.4 μmol, respectively. There were no statistical differences at $p \leq 0.05$ between vapor recoveries, liquid recoveries, and vapor/liquid recoveries for each aldehyde. The grand average pellet capacity for valeraldehyde under all conditions was 30.5 ± 3.5 μmol and that for acrolein was 27.5 ± 2.3 μmol, not statistically different at $p \leq 0.05$. The average limiting capacity for both was thus 29.0 ± 5.8 μmol or an n_m of 193 ± 39 μmol/g. The theoretical monocarbonyl capacity is 60 μmoles, n_m = 400 μmol/g. Thus, about half of the total potential capacity of the PFBHA coated pellet can actually be used, and this is suggestive of a kinetically limited uptake rate.

If aldehydes are initially physically adsorbed as vapors, the measured average aldehyde volume pellet capacity is 0.709 cm^3 or a specific volume capacity of 4.72 cm^3/g, assuming ideality.

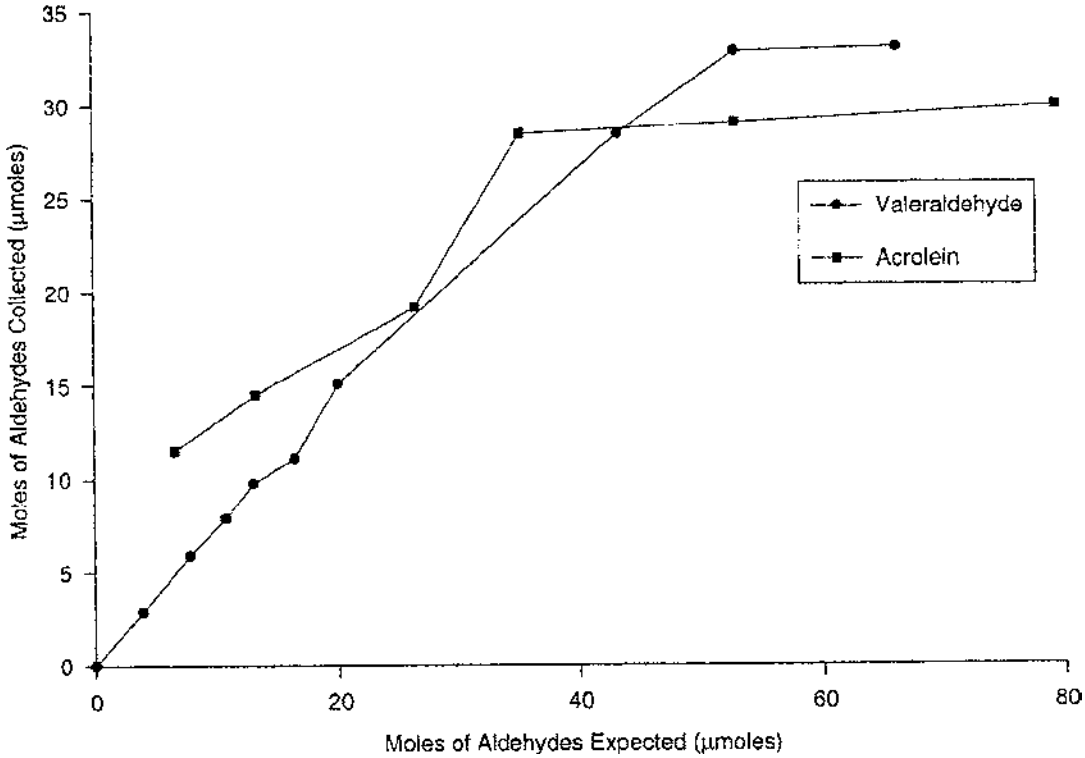

FIGURE 3

Vapor isotherm for acrolein and valeraldehyde in terms of aldehyde reacted for $R_e = 1$ for a 150 mg pellet of coated solid sorbent versus theoretical aldehyde reacted as calculated from Eq. (2) for D and then Eq. (3).

Since the pore volume of uncoated Tenax TA is about 5.43 cm^3/g by nitrogen BET analysis, an initial physical adsorption of aldehyde vapor is possible. The corresponding average liquid aldehyde pellet volumes for valeraldehyde and acrolein at saturation are 0.00322 and 0.00183 cm^3 with respective v_m of 0.0215 and 0.0122 cm^3/g.

Adsorption Isotherm Linearization Analysis

For valeraldehyde (Figure 3), a linear uptake occurred between C_A of 0.011 to 0.055 $\mu mol/cm^3$, the latter being at 46 percent of saturation after 1 hr:

$$q_A = 1730\,C_A + 0.640 \qquad R^2 = 0.9876 \qquad p \leq 0.001 \text{ for } n = 6 \quad [9]$$

The slope is 1730 ± 31 (μmol/g sorbent)/($\mu mol/cm^3$ vapor), and is related to $(k_{analyte}\ R_r\ R_e)/f$. The intercept for Eq. (9) is not significantly different from zero at $p \leq 0.05$, assuming the same RSD. Therefore, this part of the isotherm obeys Henry's Law, and R_e is close to 1. Passive sampling is thus practical up to 46 percent of pellet capacity for valeraldehyde.

For acrolein over C_A of 0.019 to 0.099 $\mu mol/cm^3$ (the latter causing about 95% saturation after 1 hr of exposure), the linear regression equation is:

$$q_A = 1330\,C_A + 47.1 \qquad R^2 = 0.9378 \qquad p \leq 0.05 \text{ for } n = 4 \quad [10]$$

The slope is 1330 ± 170 (μmol/g sorbent)/($\mu mol/cm^3$ vapor), and differs statistically from that for valeraldehyde at $p \leq 0.05$. The intercept is non-zero. The Henry's Law region is < 0.019 $\mu mol/cm^3$.

Linearization Data Analysis for Classical Isotherms

Table I presents the linearization regression equation data for the classical isotherms. All the plots were linear for both aldehydes at $p \leq 0.005$ using all data of each aldehyde (Range 1 in Table I). Acrolein was best fitted by Langmuir and BET plots at $p \leq 0.001$ with the BET linearization marginally having the highest R^2. Valeraldehyde adsorption was best characterized by Freundlich and D-R plots, with D-R being the best linearization model relative to R^2. The highest three x-axis points for the Langmuir and BET linearity plots were responsible for the linearity of the entire data set for valeraldehyde (Ranges 2 and 3 in Table I). The acrolein BET plot intercept is not statistically different from zero at $p \leq 0.001$, as were the Langmuir and BET intercepts for the three highest concentration data points for valeraldehyde. All other intercepts statistically differed from zero at $p \leq 0.05$. The BET F factors were similar at 179 ± 14 and 142 ± 13 units for valeraldehyde and acrolein, respectively; all other corresponding parameters were significantly different at $p \leq 0.05$. Freundlich linearization plots produced a slope for valeraldehyde of 0.897 and of 0.433 for acrolein, both slopes < 1 as expected.

TABLE I
Comparison of adsorption isotherm linearity plot parameters for valeraldehyde and acrolein

Aldehyde	Isotherm	Range	Linear plot regression parameters			
			Slope	Intercept	R^2	p
Valeraldehyde	Langmuir	1	$122(31) \times 10^{-5}$	$5.25(0.29) \times 10^{-4}$	0.8314	< 0.001
		2	$431(45) \times 10^{-5}$	$43(69) \times 10^{-6}$	0.9947	< 0.05
		3	$33(25) \times 10^{-5}$	$56(244) \times 10^{-5}$	0.0479	0.856
	BET	1	$165(27) \times 10^{-5}$	$1935(94) \times 10^{-7}$	0.8441	< 0.001
		2	$479(36) \times 10^{-5}$	$59(209) \times 10^{-7}$	0.9943	< 0.05
		3	$56(27) \times 10^{-5}$	$21(111) \times 10^{-5}$	0.1228	0.483
	Freundlich	1	0.897(0.037)	7.096(0.115)	0.9881	< 0.001
	D-R	1	−0.2914(0.0098)	6.273(0.068)	0.9921	< 0.001
Acrolein	Langmuir	1	$399(38) \times 10^{-5}$	$201(46) \times 10^{-6}$	0.9658	< 0.001
	BET	1	$417(38) \times 10^{-5}$	$29(70) \times 10^{-6}$	0.9671	< 0.001
	Freundlich	1	0.433(0.060)	6.056(0.164)	0.9306	< 0.005
	D-R	1	−0.120(0.016)	5.90(0.14)	0.9343	< 0.005

BET, Brunauer-Emmett-Teller; D-R, Dubinin-Radushkevich; Range 1, all data; Range 2, highest three data for x-axis; Range 3, all data except range 2 data; slope and intercept data are in appropriate units and provided as arithmetic mean and standard deviation; R^2, square of the correlation coefficient; p, statistical probability of non-linearity using Student's t.

Langmuir Adsorption Isotherm: $C_A/q_A = C_A/n_m + 1/(bn_m)$ where C_A is the concentration of adsorbate in the vapor phase (mol/cm^3), q_A is the moles adsorbed/g sorbent, n_m is the mole of adsorbate/g for single occupation of all sites, and b is the Langmuir constant (cm^3/mol).

BET Adsorption Isotherm: $z/(1-z)q_A = (F-1)z/Fn_m + 1/Fn_m$ where z is the reduced pressure, and F is the BET constant.

Freundlich Adsorption Isotherm: $\ln q_A = \ln K + 1/n \ln C_A$ where K is the Freundlich preexponential factor, and n is the Freundlich exponential factor.

Dubinin-Radushkevich Adsorption Isotherm: $\ln q_A = \ln n_m - (k''R^2T^2 \ln^2 z^{-1})/\gamma^2$ where $n_m = W^*/V_l$ where W^* is the limiting potential specific volume (ml/g) at temperature T in K, V_l is the liquid molar volume (ml/mol), k'' is a constant (energy^{-2}), γ is the affinity coefficient, and R is the gas constant in appropriate units.

Table II presents the n_m and v_m calculated from Table I for three classical adsorption isotherms. The Langmuir slope for all the valeraldehyde data (Range 1) was 0.00122 ± 0.00031 g/μmole. Therefore, n_m is $1/(0.00122 \pm 0.00031) = 820 \pm 210$ μmol/g (Table II), with poor precision (CV = 26%). If only the three highest concentration points are regressed (Range 2 in Table I), the slope is 0.00431 ± 0.00045 g/μmol, and its n_m of 232 ± 24 μmol/g is not significantly different from the measured 203 ± 21 μmol/g. The same analysis using BET linearization yielded respective n_m values of 622 ± 100 and 210 ± 16 μmol/g (Table II). Neither of these values differed significantly from the corresponding Langmuir n_m at $p \leq 0.05$. For acrolein, there was also no significant difference between the corresponding Langmuir and BET n_m (Table II). This behavior for both aldehyes is expected if a BET I isotherm is equivalent to the Langmuir isotherm. The D-R analysis produced n_m of 530 ± 36 and 365 ± 52 μmol/g for valeraldehyde and acrolein, respectively, statistically different from each other at $p \leq 0.05$.

The isotherm n_m range is between 1.1–4.0 times the measured n_m, and 0.58–2.1 times the theoretical n_m. No isotherm that utilized all the experimental data predicted experimental saturation n_m even for $p \leq 0.001$ linearity. The BET isotherm came closest for acrolein.

TABLE II
Comparison of sorbent capacity terms for three adsorption isotherms for valeraldehyde and acrolein (parameters are defined in Table I)

Aldehyde	Isotherm	Range	Capacity (μmol/g)	Liquid aldehyde capacity (μl/g)
Valeraldehyde	Langmuir	1	820(210)[A]	86(22)[A]
		2	232(24)	24.4(2.5)
	BET	1	622(100)[A]	46.1(7.4)[A]
		2	210(16)	22.1(1.7)
	D-R	1	530(36)[A]	39.1(2.7)[A]
	Experimental		203(21)	21.5(2.2)
Acrolein	Langmuir	1	251(24)[A]	16.7(1.6)[A]
	BET	1	242(22)[A]	16.1(1.5)[A]
	D-R	1	365(52)[A]	24.3(3.5)[A]
	Experimental		183(15)	12.2(1.0)

[A]Significantly different from experimental value at Student's t at $p \leq 0.05$.

Calculation of activation energy was only possible for the BET F parameter.

$$F = g_0 \exp[-(\Delta H_1 - \Delta H_L)/RT] \quad [11]$$

where ΔH_1 is the enthalpy of adsorption of the first layer, and ΔH_L is the heat of liquefaction or solidification at temperature T in K, with g_0 being the entropic factor, the latter usually being set equal to 1.0. BET Type II and IV adsorption isotherms occur for $\Delta H_1 > \Delta H_L$, and BET Types III and V for $\Delta H_1 < \Delta H_L$. For a BET Type I isotherm, $\Delta H_L = 0$.

The simplest model is BET I since it assumes a monolayer for both physical adsorption and chemisorption and there is no explicit assumption of a liquid layer. Since $F = 179 \pm 14$ and 142 ± 13 for valeraldehyde and acrolein, at $g_0 = 1$ the respective ΔH_1 values are 15.2 ± 1.2 and 14.5 ± 1.3 kJ/mol. Such energies are not characteristic of covalent bond energies but are more like energies for physical adsorption and hydrogen bonding that range from 13 to 32 kJ/mol.[22] Since carbonyl bond energy is enhanced by conjugation in acrolein increasing to 773 kJ/mol from 670 kJ/mol mostly in the π-bond component,[27] acrolein chemisorption is expected to be more energetic than for valeraldehyde if the addition reaction is the rate determining step. This is not so. For BET II–V models, the respective ΔH_L energies are 34.0 and 31.3 kJ/mol calculated from the Clausius-Clapeyron equation. The calculated respective ΔH_1 values are 18.8 and 16.8 kJ/mol for all the data for each aldehyde. The ΔH_1 for the high concentration range for valeraldehyde is 22 kJ/mol. Thus BET III or V behavior is supported for a multilayer adsorption process. Since these BET types II–V calculations assume liquid aldehyde layers, the low enthalpy values are expected. No literature data exist for g_o which is usually obtained through temperature measurements. There is no temperature dependence of $(k_{analyte}\ R_r\ R_e)/f$ between 4–48°C,[14] a characteristic of adsorptions described by the D-R isotherm, which has no activation energy parameter.

Addition Reaction, Bond Energies and Bond Lengths

The adsorption model is:

$$\underset{\text{Outside Environment}}{\text{Analyte}_{(vapor)}} \leftrightarrow \underset{\text{Inside Membrane}}{\text{Analyte}_{(vapor)}} \leftrightarrow \underset{\text{Pellet Surface}}{\text{Analyte}_{(physically\ adsorbed)}} \leftrightarrow \underset{\text{Pellet Micropores}}{\text{Analyte}_{(activated)}} \rightarrow\rightarrow \underset{\text{Pellet Solid Product}}{\text{O-oxime}} \quad [12]$$

For the last step of Eq. (12) and assuming carbonyl nucleophilic addition chemistry,[29] the trigonal carbonyl group (bond length 120–122 pm; bond energy of about 670 kJ/mol)[27] reacts with one molecule of PFBHA to form several tetrahedral intermediates, an alkoxyiminium ion, and on loss of a proton, the O-oxime,[29] Eq. (13):

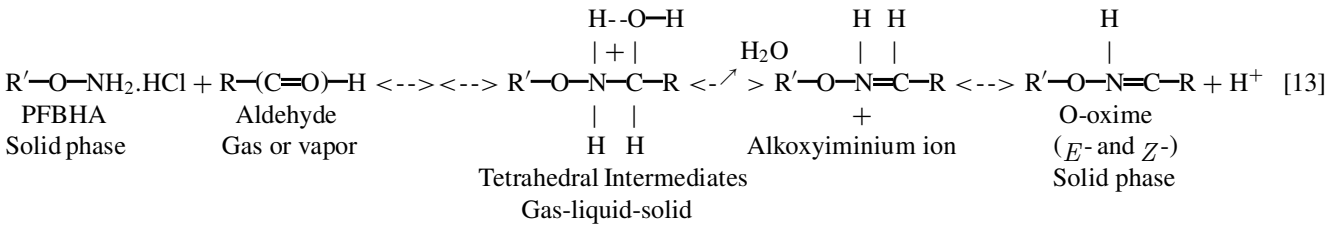

[13]

where R′ is the (2,3,4,5,6-pentafluorobenzyl) group; R is an alkyl, aryl, or alicyclic group.

The tetrahedral intermediate in Eq. (13) is just one of many possible but is the most stable one. Its σ C—O bond has an energy of about 340 kJ/mol. The bond lengths in pm are: C—O, 143; O—H, 95.6; C—H, 109.6; C—C, 154; C—N, 147. The various angles are HCO 108.9°, HCH 123.55°, and CCH 109.5°. The hydrogen bonds have energies of 13–32 kJ/mol.[27] The tetrahedral intermediates all have weak hydrogen bonds as does the oxime product.[30] The RCH[(O)H—N] bond is about 216 pm and 14.3 kJ/mol.[29] The RCH[(O)H—O] bond is 193 pm and 29.1 kJ/mol for the *E*-form, and 190–205 pm and 21.7–31.6 kJ/mol for the *Z*-form. The intramolecular H-bond lengthens from 207 to 240 pm on protonation, and its strength decreases. In the O-oxime product, the N=C bond length is about 128 pm.

The actual addition process is usually visualized in two ways[29]: the carbonyl group and the electron pair of a strong nucleophile first form a tetrahedral oxyanion, which is further protonated twice at the oxygen, and then dehydrated to produce O-oxime. The other mechanism involves acid catalysis to protonate the carbonyl group first to give an oxonium ion, whose carbon accepts the electron pair of a weak nucleophile to produce the first tetrahedral intermediate, with a hydrogen on the bonded nucleophile being then removed by a base to form the aminoalcohol. Acid catalysis is important in solution.[31]

PFBHA, like other hydroxylamine hydrochloride salts, can form a lattice with strong hydrogen bonds and can donate protons to a suitable acceptor molecule like an aldehyde that can reciprocate with a donated electron but not a proton.[29] Having PFBHA molecules in close proximity in a solid coating may

facilitate proton donation to form an activated oxonium ion. Efficient reaction due to the orienting effect of the surface PFBHA molecules may also occur. Since only about half the theoretical capacity is actually available for reaction, the minimum number of PFBHA molecules for a chemisorptive receptor site may be at least two.

The fluorinated benzyl group of PFBHA may be held by the flat aromatic rings of the Tenax TA surface, with the oxyamino hydrochloride end sticking out from the surface. Rotation will occur about its σ C—O, O—N, and N—H bonds. The bond lengths expected in pm are[27]: C═C, 139; C—F, 135; ring C-sidechain C, 150; C—H, 111; C—O, 141; O—N, 124; and N—H, 103. The electronegative ring fluorines will enhance the inductive effect of the sidechain oxygen lone pairs, strengthening the C—O and O—N σ-bonds relative to isolated ones and weakening the N—H bonds. Thus dimeric PFBHA sites could be ready to donate at least one proton to produce an activated protonated aldehyde. The existence of an extrinsic precursor[32,33] would allow lateral diffusion of aldehyde on the surface to increase the opportunity to find a free site for reaction. The activation and surface diffusion processes would then be under kinetic control. This could explain the high efficiency of the chemisorption, and the apparent low activation energy.

Microporosity Considerations

The Tenax TA pellet of path width w cm is microporous. Tenax TA pores are filled with PFBHA coating molecules. A modification of Eq. (1) is used to describe diffusion control uptake of analyte into microporous surfaces:[34]

$$Fl_1 = (D/L)(C_{air} - C_{surf}) \quad [14]$$

where Fl_1 is the average flux of analyte to the actual sorbent surface area in mol cm^{-2} s^{-1}, and C_{surf} is the concentration of analyte at the pellet surface, and

$$Fl_2 = (\zeta \in D)\, dC/dx \quad [15]$$

$$= (wD/\alpha L)dC/dx \quad [16]$$

where Fl_2 is the average flux of analyte from the sorbent outer surface into its interior adsorbing area in mol cm^{-2} s^{-1}; ζ is the dimensionless tortuosity factor for interparticle diffusion within the pellet; $\in$ is the dimensionless fractional interparticle void volume within the pellet; x is the distance from the pellet surface into its interior for adsorption; and α is the mass transfer resistance, $w/\zeta \in L$.

The area of adsorption for microporous sorbents is defined not only by sampler dimensions, Eqs. (1) and (7), but also by micropore number and micropore size distribution. The surface area A in Eqs. (1), (3), (7), and (8) is replaced by the actual micropore surface area found from a BET I surface area analysis linearization, and is used to calculate Fl_1 and Fl_2.

$$Fl_2/Fl_1 = (\zeta \in L)(dC/dx)/(C_{air} - C_{surf})$$

$$= w(dC/dx)/[\alpha(C_{air} - C_{surf})] \quad [17]$$

At steady-state $Fl_1 = Fl_2$

$$\zeta \in L\, dC/dx = (C_{air} - C_{surf}) = w(dC/dx)/\alpha \quad [18]$$

If C_{surf} is close to zero,

$$\zeta \in L\, dC/dx = C_{air} = w(dC/dx)/\alpha \quad [19]$$

$$dC/C_{air} = dx/\zeta \in L = \alpha dx/w \quad [20]$$

Integrating between the surface and the average distance x for which vapor penetration occurs from near the surface at which $x = 0$ at concentration C_{air},

$$\ln(C_x/C_{air}) = x/\zeta \in L = \alpha\, x/w = k_m\, x \quad [21]$$

where x/w is the reduced distance and w should be constant.

Thus the constant k_m, the microporous adsorptivity coefficient in cm^{-1}, is $(1/\zeta \in L = \alpha/w)$, and C_x varies exponentially with distance x away from the original exposure surface, often a micropore.

Mass transfer to within the sorbent pellet is related to the internal pellet concentration:[34]

$$\zeta D(d^2C/dx^2) = [(1- \in)K/\in +1]dC/dt \quad [22]$$

where concentration equilibrium is assumed between the interparticle void space of macropores, mesopores, and micropores and their adsorbing surfaces with which they are in contact. K is the partition coefficient in mol of analyte/cm^3 of sorbent per mol of analyte/cm^3 vapor for the initial physical adsorption assuming a Henry type law.

Chemisorption can be factored into K by multiplying it by the reaction efficiency R_r, the fraction of available analyte molecules in contact with the surface that react (Eq. 7).

$$\zeta D(d^2C/dx^2) = [(1- \in)KR_r/\in +1]dC/dt \quad [23]$$

The sampler uptake dn/dt without chemisorption is the sum of the moles in the air gap, plus those within, and on the sampling pellet collected over sampling time t:

$$dn/dt = \text{uptake} = C_{air}AD/(L + wn_{air}/\zeta \in n_{max})$$

$$= C_{air}AD/(L + \propto n_{air}/Ln_{max}) \quad [24]$$

From Eq. (22),

$$(dC/dt)/(dn/dt)$$

$$= 1/dV = \zeta C_{air} \propto^2 (L + \propto n_{air}/Ln_{max})/\{Aw^2[(1- \in)K/\in +1]\}$$

$$= C_{air}(L + \propto n_A/Ln_{max})/\{\zeta \in^2 L^2[(1- \in)K/\in +1]\} \quad [25]$$

dV is the volumetric sampling constant of the passive sampler in terms of parameters relating to the microporous nature of the

passive sampler. Equation (25) is essentially a first order relationship with a complex first order rate constant. The linearization relationships for the Langmuir and BET I isotherms would be observed for such a relationship.

Adding chemisorption as a factor replaces K with KR_r in Eq. (25) and does not change the above conclusions if R_r is constant:

$$\begin{aligned}&(dC/dt)/(dn/dt)\\&= 1/dV = \zeta C_{air}\alpha^2 (L+ \propto n_{air}/Ln_{max})/\{Aw^2[(1- \in)KR_r/\in +1]\}\\&= C_{air}(L+ \propto n_A/Ln_{max})/\{\zeta \in^2 L^2[(1- \in)KR_r/\in +1]\}\end{aligned} \quad [26]$$

If the adsorption kinetics instead obey:[34]

$$d^2C/dx^2 = 1/(\zeta D)[(1- \in)K/\in +1]dC/dt \quad [27]$$

$$= (\in \alpha L/wD)[(1- \in)K/\in +1](dC/dt) \quad [28]$$

When $Fl_1 = Fl_2$ and using Eq. (15),

$$dC/C^2 = Ddt/\{\zeta\in^2 L^2[(1- \in)K/\in +1]\} \quad [29]$$

On integrating this second order kinetic equation from $t = 0$ to time t,

$$1/C_t = 1/C_o - Dt/\{\zeta\in^2 L^2[(1- \in)K/\in +1]\} \quad [30]$$

with a second order rate constant of $D/\{\zeta\in^2 L^2[(1 - \in) K/\in +1]\}$.

For a microporous process that also involves chemisorption, Eq. (30) becomes:

$$1/C_t = 1/C_o - Dt/\{\zeta \in^2 L^2[(1- \in)KR_r/\in +1]\} \quad [31]$$

with a second order rate constant of $D/\{\zeta\in^2 L^2[(1 - \in) KR_r/\in +1]\}$.

For microporous physical adsorption at low z or reduced pressure, the D-R adsorption isotherm predicts the same results as does an irreversible adsorption isotherm when K is high (physical adsorption and chemisorption), or when $\alpha < 0.5$. Chemisorption activated by the collisional energy involved with physical adsorption may permit high K and low activation energies. This process is the same energetically as activated adsorption involving an extrinsic precursor referred to above.[32,33]

Microporosity may explain why the linearization procedures for the four classical isotherms are all observed, and why not all the available reaction sites can be used. However, it is hard to assess how the model performs quantitatively because most of the values for the parameters are unknown. Thus, $\zeta\in$ in Eq. (15), α in Eq. (16), K in Eq. (22), as well as R_r and R_e not being constant, or a mixture of all of these may be important. For example, assuming R_r is constant and $R_e = 1$, if $\zeta\in$ is 0.5, α is 0.546 for $w/L = 0.273 \pm 0.012$, with a minimum CV of 4.4 percent. Then k_m in Eq. (21) is about 0.182 cm^{-1}. Clearly, much work is still required to assess how important microporosity is and why the addition reaction is not the rate limiting step for this chemisorption.

CONCLUSIONS

No classical adsorption isotherm (Langmuir, BET, Dubinin-Radushkevich, Freundlich) predicted pellet capacity, even though all the data could be linearized appropriately by each isotherm. Dividing the data into linearization regions achieved capacity predictability but empirically only. The published passive sampling region for valeraldehyde extends up to 46 percent of pellet saturation but lies below 18 percent saturation for acrolein. Passive sampling between 18 to 95 percent saturation for acrolein is possible with a different linear equation from that used below 18 percent saturation where a Henry's law type sampling constant is descriptive. A microporosity model, the presence of an extrinsic precursor, and a requirement for two derivatizing molecules per reactive site accounted for most of the qualitative results. Industrial hygienists who depend on sampling constants determined in the laboratory by developers of the passive sampler should not expose their diffusive samplers to conditions that cause near saturation of the sampling element or cause departures from Henry's Law behavior. Diffusive samplers that also work by chemisorption also may require understanding of the chemical processes that are operating to allow interpretation of air sampling results, particularly the influence of reaction efficiencies, chemisorption efficiency relative to physical adsorption, and the applicability of Fick's First Law to the situation in addition to the usual effects of temperature, RH, and intermittent sampling.

ACKNOWLEDGMENTS

NIOSH/CDCP Grant 5 RO1 OH03120 and the UCLA Center for Occupational and Environmental Health were responsible for financial support.

REFERENCES

1. Carlier, P.; Hannachi, H.; Mouvier, G.: The Chemistry of Carbonyl Compounds in the Atmosphere—A Review. Atmos Environ 20:2079–2099 (1986).
2. Otson, R.; Fellin, P.: A Review of Techniques for Measurement of Airborne Aldehydes. Sci Tot Environ 77:95–131 (1988).
3. Wagner, T.; Wyszynski, M.L.: Aldehydes and Ketones in Engine Exhaust Emissions—A Review. Proc Inst Mech Engin 210:109–122 (1996).
4. Eller, P.M., Ed.: NIOSH Manual of Analytical Methods, 3rd ed., Methods 2501, 2526, 2529, 2531, 2538, 2539, and 2541. NIOSH, Cincinnati, OH (1989).
5. Occupational Safety and Health Administration (OSHA): OSHA Analytical Methods Manual: Methods 68 and 52. OSHA: U.S. Department of Labor, Salt Lake City (1990).

6. U.S. Environmental Protection Agency (EPA): Technical Assistance Document for Sampling and Analysis of Toxic Organic Compounds in Ambient Air; EPA-600/8-90-005. EPA, Washington, DC (1990).
7. Wu, L.-J.; Que Hee, S.S.: A Solid Sorbent Personal Air Sampling Method for Aldehydes. Am Indus Hyg Assoc J 56:362–367 (1995).
8. Shen, Y.; Que Hee, S.S.: Optimization of a Solid Sorbent Dynamic Personal Air Sampling Method for Aldehydes. Appl Occup Environ Hyg 15:228–234 (2000).
9. Cassinelli, M.E.; Hull, R.D.; Crable, J.V.; Teass, A.W.: Protocol for the Evaluation of Passive Monitors. In: Diffusive Sampling: An Alternative Approach to Workplace Air Sampling, A. Berlin, R.H. Brown, K.J. Saunders, Eds., pp. 190–202. Royal Society of Chemistry: London, United Kingdom (1987).
10. Levin, J.-O.; Lindahl, R.; Andersson, K.: Monitoring of Parts-per-Billion Levels of Formaldehyde. J Air Pollut Control Assoc 39:44–47 (1989).
11. Noble, J.S.; Strang, C.R.; Michael, P.R.: A Comparison of Active and Passive Sampling Devices for Full-Shift and Short-Term Monitoring of Formaldehyde. Am Indus Hyg Assoc J 54:723–732 (1993).
12. Mulik, J.D.; Lewis, R.G.; McClenny, W.A.: Modification of a High Efficiency Passive Sampler to Determine Nitrogen Dioxide or Formaldehyde in Air. Anal Chem 61:187–189 (1989).
13. Levin, J.-O.; Lindahl, R.: Diffusive Air Sampling of Reactive Compounds: A Review. Analyst 119:79–83 (1994).
14. Tsai, S.-W.; Que Hee, S.S.: A New Passive Sampler for Workplace Aldehydes. Am Indus Hyg Assoc J 60:463–473 (2000).
15. Tsai, S.-W.; Que Hee, S.S.: A New Passive Sampler for Regulated Workplace Aldehydes. Appl Occup Environ Hyg 14:255–262 (2000).
16. Brown, R.H.; Purnell, C.J.: Collection and Analysis of Trace Organic Vapor Pollutants in Ambient Atmospheres: The Performance of a Tenax-GC Adsorbent Tube. J Chromatogr 178:79–90 (1979).
17. Pankow, J.F.: Gas Phase Retention Volume Behavior of Organic Compounds on the Sorbent Poly(oxy-m-terphenyl-2′,5′-ylene). Anal Chem 60:950–958 (1988).
18. Helmig, D.; Vierling, L.: Water Adsorption Capacity of the Solid Sorbents Tenax TA, Tenax GR, Carbotrap, Carbotrap C, Carbosieve SIII, and Carboxen 569 and Water Management Techniques for the Atmospheric Sampling of Volatile Organic Trace Gases. Anal Chem 67:4380–4386 (1995).
19. Gorecki, T.; Martos, P.; Pawliszyn, J.: Strategies for the Analysis of Polar Solvents in Liquid Matrixes. Anal Chem 70:19–27 (1998).
20. Martos, P.A.; Pawliszyn, J.: Sampling and Determination of Formaldehyde Using Solid-Phase Microextraction with On-Fiber Derivatization. Anal Chem 70:2311–2320 (1998).
21. Supelco: SPME Applications Guide, Bulletin 925. Bellefonte, PA (1999).
22. Adamson, A.W.: Physical Chemistry of Surfaces, 4th ed., pp. 601–647. John Wiley and Sons, New York (1982).
23. Fuller, E.N.; Schettler, P.D.; Giddings, J.C.: A New Method for Prediction of Binary Gas-Phase Diffusion Coefficients. Indus Eng Chem 58:19–27 (1966).
24. 3M: 3M Organic Vapor Monitors #3500/3510 Instructions for Use, 3M Occupational Health and Safety Products Division, Publication 34-7020-1249-2. 3M, St. Paul, MN (1996).
25. 3M: 3M Organic Vapor Monitor Sampling and Analysis Guide: Organic Vapor Monitors 3500/3510 and Organic Vapor Monitors 3520/3530. 3M Occupational Health and Environmental Safety Division Publication 70-0702-1914-5 RPI. 3M, St. Paul, MN (1996).
26. Snedecor, G.W.; Cochran, W.G.: Statistical Methods, 8th ed. Iowa University Press, Ames, IA (1989).
27. Berthier, G.; Serre, J.: In: The Chemistry of the Carbonyl Group, S. Patai, Ed., pp. 1–77. Interscience, New York (1966).
28. Verschueren, K.: Handbook of Environmental Data on Organic Chemicals. Van Nostrand Reinhold, New York (1983).
29. Solomons, T.W.G.: Organic Chemistry, 6th ed., pp. 716–731. John Wiley and Sons, New York (1996).
30. Oscik, J.; Cooper, I.L.: Adsorption. Halsted Press, New York (1982).
31. Cancilla, D.A.; Chou, C.C.; Barthel, R.; Que Hee, S.S.: Characterization of the O-(2,3,4,5,6-Pentafluorobenzyl)hydroxylamine Hydrochloride (PFBOA) Derivatives of Some Aliphatic Mono- and Di-Aldehydes and Quantitative Water Analysis of These Aldehydes. J Assoc Offic Anal Chem Int 75:842–854 (1992).
32. Doren, D.J.; Tully, J.C.: Precursor-Mediated Adsorption and Desorption: A Theoretical Analysis. Langmuir 4:256–268 (1988).
33. Doren, D.J.; Tully, J.C.: Dynamics of Precursor-Mediated Chemisorption. J Chem Phys 94:8428–8440 (1991).
34. Adley, D.P.; Underhill, D.W.: Fundamental Factors in the Performance of Diffusive Samplers. Anal Chem 61:843–847 (1989).